EFFECT OF DISPERSED-PHASE VISCOSITY ON THE MAXIMUM STABLE DROP SIZE FOR BREAKUP IN TURBULENT FLOW

KUNIO ARAI, MIKIO KONNO, YUICHI MATUNAGA AND SHOZABURO SAITO
Department of Chemical Engineering, Tohoku University, Sendai 980

A formula for the maximum stable drop size has been derived theoretically, by taking into consideration the effect of the dispersed-phase viscosity. The derived formula indicates that the controlling factors of the maximum stable drop size are the Weber Number and the viscosity group which is defined as the ratio of the viscous stress to the stress of interfacial tension. The validity of the formula was confirmed experimentally over a wide range of dispersed-phase viscosity.

Introduction

The agitation of two or more liquid phases in tanks is a common operation in the chemical industry. In some operations it is often desirable to have realistic information with regard to the size of drops which are formed in the agitated tank. The knowledge of the breakup of a drop in turbulence is essential for determining the drop sizes; the maximum stable drop size is especially important for elucidating the mechanism of a drop breakup and for its theoretical treatment.

Hinze[2] suggested that the breakup of a drop occurs when the Weber Number $N_{We}=\rho_c\bar{u}^2(d)d/\sigma$ reaches a critical value $(N_{We})_{crit}$. Namely, the size of the maximum stable drop, d_{max}, can be determined by solving the following equation.

$$\rho_c\bar{u}^2(d_{max})d_{max}/\sigma=(N_{We})_{crit}(=\text{const.}) \quad (1)$$

This equation is adequate, when the stress due to the interfacial tension counteracts the deformation of the drop. On the other hand, viscous stress due to internal flow will also prevent the deformation of the drop. Hinze also analyzed the effect of the dispersed-phase viscosity on $(N_{We})_{crit}$ when the dynamic pressure in a drop was of the same order of magnitude as the external stress acting on the drop surface. On the basis of Hinze's analysis Hughmark[3] proposed the equation for the maximum stable drop size, which included the viscosity effect.

However, these treatments will be invalid as the dispersed-phase viscosity increases, because the dynamic pressure in a drop becomes smaller than the external stress and the viscous stress in a drop becomes of the same order of magnitude as the external stress. The present work proposes a more general expression for d_{max} which is applicable in the wide range of the dispersed-phase viscosity.

Received October 2, 1976. Correspondence concerning this article should be addressed to S. Saito.

1. The Maximum Stable Drop Size for Breakup in Isotropic Turbulence

Assuming that the turbulence is isotropic and that the drop diameter d is much larger than the Kolmogoroff length η, the mean square velocity difference $\bar{u}^2(d)$ is given by

$$\bar{u}^2(d)\propto(\varepsilon d)^{2/3} \quad (2)$$

Introducing Eq. (2) into Eq. (1), Hinze[2] obtained the following equation.

$$\rho_c\varepsilon^{2/3}d_{max}^{5/3}/\sigma=\text{const.} \quad (3)$$

In these equations ε is the energy dissipation rate per unit mass and for a fully baffled turbine operating at high Reynolds number it is given as follows:

$$\varepsilon\propto n_r^3L^2 \quad (4)$$

Introducing Eq. (4) into Eq. (3) Shinnar[6] has derived the following equation for the maximum stable drop size, d_{max},

$$d_{max}/L=\text{const.}\ (\rho_c n_r^2L^3/\sigma)^{-0.6} \quad (5)$$

This equation gives good results only when the drop diameter d is much larger than the Kolmogoroff length and the dispersed-phase viscosity μ_d is sufficiently small, i.e., less than of the order of 10 cp. Larger values of μ_d play an important part in resisting the deformation of a drop and make Eqs. (3) and (5) inappropriate[2,7]. In the present work this effect of the dispersed-phase viscosity is introduced into the expression for the maximum stable drop size as follows. As the stress due to the interfacial tension counteracts

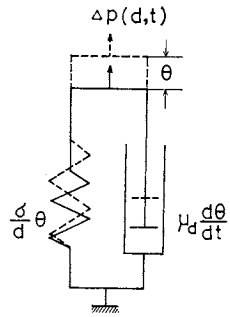

Fig. 1 Voigt model for the deformation of a drop

the deformation of a drop in an elastic manner, it may be assumed that the deformation is represented by the Voigt model, shown in **Fig. 1.** In this model the modulus of a spring equals σ/d, and an internal viscosity in a dashpot equals μ_d.

If a stress F is now applied to the model in Fig. 1, the applied stress F must equal the opposing stress in the spring $(\sigma/d)\theta$ plus the viscous stress $\mu_d(d\theta/dt)$; that is,

$$F=(\sigma/d)\theta+\mu_d(d\theta/dt) \tag{6}$$

where θ is the spring elongation. In our presentation θ represents the deformation of the drop and F the dynamic pressure difference of turbulent motions which acts on the surface of the drop. Since F is the quantity which fluctuates with time and depends on the drop size, it can be written as;

$$F=\Delta P(d,t) \tag{7}$$

In order to solve Eq. (6) exactly, it is necessary to know $\Delta P(d,t)$ in all details as a function of time. Because of the irregularity of turbulence this can not be done; however, $\Delta P(d,t)$ can be described by laws of probability. Namely, it is possible to give distinct average values of the magnitude and the period of $\Delta P(d,t)$. Designating these average values to $\overline{\Delta P}$ and T, respectively, they are given for the region of turbulence with which the present work is concerned as follows:

$$\overline{\Delta P}\propto\rho_c\overline{u^2}(d)\propto\rho_c(\varepsilon d)^{2/3} \tag{8}$$

$$T\propto d^{2/3}/\varepsilon^{1/3} \tag{9}$$

In the first approximation, the expression "pseudo turbulence" is used in order to characterize the deformation of a drop in turbulence: this refers to hypothetical case of a flow field with a regular pattern that shows a distinct constant periodicity in time and space. Accordingly, $\Delta P(d,t)$ is a periodic function whose magnitude and period are proportional to $\overline{\Delta P}$ and T as given by Eqs. (8) and (9). Then, $\Delta P(d,t)$ will be given as follows:

$$\Delta P(d,t)=\overline{\Delta P}g(\omega) \tag{10}$$

where

$$\omega=t/T \tag{11}$$

In this equation $g(\omega)$ is a universal periodic function which depends only on ω. The universality of $g(\omega)$ results from the consideration that the quantities of $\overline{\Delta P}$ and T are main factors which determine the statistical property of $\Delta P(d,t)$.

Using Eqs. (10) and (11), Eq. (6) can be transformed into the following dimensionless form;

$$\theta+C_1N_{vi}(d\theta/d\omega)=C_2N_{We}g(\omega) \tag{12}$$

where

$$N_{vi}=\mu_d\varepsilon^{1/3}d^{1/3}/\sigma \tag{13}$$

$$N_{We}=\rho_c\overline{u^2}(d)d/\sigma \tag{14}$$

and C_1 and C_2 are constants. N_{vi} is called the viscosity group. It is the same notation that Hinze[2] used for the dimensionless group $\mu_d/\sqrt{\rho_d\sigma d}$, because both groups account for the effect of the viscosity of the liquid in a drop.

Equation (12) has a solution of the following form.

$$\theta=\theta_{\omega=0}\exp(-\omega/C_1N_{vi})+C_2N_{We}I(\omega,N_{vi}) \tag{15}$$

where I is a function of ω and N_{vi} and is given by the following equation.

$$I(\omega,N_{vi})=\frac{1}{C_1N_{vi}}\exp(-\omega/C_1N_{vi})\int_0^{\omega}g(\omega)\exp(\omega/C_1N_{vi})d\omega \tag{16}$$

Since the first term on the right-hand side in Eq. (15) vanishes rapidly with time, it can be ignored in this case. Consequently, θ is described as

$$\theta=C_2N_{We}I(\omega,N_{vi}) \tag{17}$$

As seen from Eq. (17) θ reaches a maximum value, θ_{max}, when the value of I becomes maximum. At a maximum point the following equation is satisfied.

$$dI(\omega,N_{vi})/d\omega=0 \tag{18}$$

and apparently the value of I at the maximum point depends only on N_{vi}. Hence the maximum deformation θ_{max} can be expressed as

$$\theta_{max}=C_2N_{We}I_{max}(N_{vi}) \tag{19}$$

where I_{max} is an unknown function which depends on N_{vi}, because the functional form of $g(\omega)$ cannot be determined explicitly. However, as N_{vi} becomes very small or very large, the limits of I_{max} can be derived by means of Eq. (12). When N_{vi} approaches zero, Eq. (12) is simplified to

$$\theta=C_2N_{We}g(\omega) \tag{20}$$

The maximum value of $g(\omega)$ is regarded as a universal constant and therefore,

$$\lim_{N_{vi}\to0}\theta_{max}=\text{const. } N_{We} \tag{21}$$

By comparing the above equation with Eq. (19), we obtain

$$\lim_{N_{vi}\to0}I_{max}=\text{const.} \tag{22}$$

When N_{vi} is limited to infinity, we obtain in the same way as above the following equation.

$$\lim_{N_{vi}\to\infty} I_{max}=\text{const. } N_{vi}^{-1} \tag{23}$$

For convenience, if a function $f(N_{vi})$ is defined as

$$I_{max}(N_{vi})\equiv\text{const.}/\{1+f(N_{vi})\} \tag{24}$$

Equations (22) and (23) can be rewritten as

$$\lim_{N_{vi}\to 0} f(N_{vi})=0 \tag{25}$$

$$\lim_{N_{vi}\to\infty}(1+f(N_{vi}))=\text{const. } N_{vi} \tag{26}$$

It is, now, assumed that the breakup of a drop occurs when θ_{max} reaches a certain critical value θ_{crit}.

The expression of the maximum stable drop size d_{max} is, then, obtained by using Eqs. (2), (14), (19) and (24) as

$$\rho_c\varepsilon^{2/3}d_{max}^{5/3}/\sigma(1+f(N_{vi}))=\text{const.} \tag{27}$$

where

$$N_{vi}=\mu_d\varepsilon^{1/3}d_{max}^{1/3}/\sigma \tag{28}$$

When the effect of the dispersed-phase viscosity μ_d is neglected, i.e., $N_{vi}\to 0$, Eq. (27) agrees with Eq. (3) derived by Hinze. On the other hand, when the effect of μ_d is sufficiently large, i.e., $N_{vi}\to\infty$, Eq. (27) can be transformed by using Eqs. (26) and (28) into the form;

$$\rho_c\varepsilon^{1/3}d_{max}^{4/3}/\mu_d=\text{const.} \tag{29}$$

Substituting Eq. (4) into the above equation, we obtain the following relation between d_{max} and the operation variables for the region of high dispersed-phase viscosity.

$$d_{max}/L=\text{const. } (\rho_c n_r L^2/\mu_d)^{-0.75} \tag{30}$$

This is the same equation as the one proposed previously by means of dimension analysis[4].

In the medium region, where both the interfacial-tension force and the viscous stress must be taken into account, it is necessary for expressing the relation between d_{max} and the operation variables explicitly that the functional form of $f(N_{vi})$ is predetermined experimentally.

2. Experiment

2. 1 Apparatus

A schematic diagram of the equipment is shown in **Fig. 2**. The mixing vessel was a glass cylinder of 12.7 cm i.d. and 12.7 cm height, enclosed by stainless steel plates. The impeller was a six-blade disk turbine centered vertically in the vessel. Four equally spaced baffles, each one-tenth the diameter of the vessel in width, were installed. The square tank surrounding the vessel served as a constant-temperature bath. In addition, it allowed pictures to be taken through the cylindrical vessel without optical distortion.

2. 2 Procedure

Polystyrene–*o*-xylene solutions ranging in polystyrene concentration from 0 to 25 wt% were dispersed in water to which a small amount of polyvinyl alcohol had been added in order to prevent adhesion of drops to the wall of the vessel. The continuous phase was saturated with *o*-xylene prior to each run. All runs were made in a completely filled vessel in order to avoid complication which would result from introduction of a third (gas) phase into the liquid. Dispersed phase volume fraction ϕ was always taken below 0.3%, in order to satisfy sufficiently noncoalescing conditions[8]. Properties of the continuous and dispersed phase liquids and the experimental conditions are summarized in **Tables 1** and **2**. Interfacial tensions were determined by the method of pendant drops and their values 22($\pm$0.4) dyne/cm were independent of the polystyrene concentration in the dispersed phase. Viscosities were measured with a

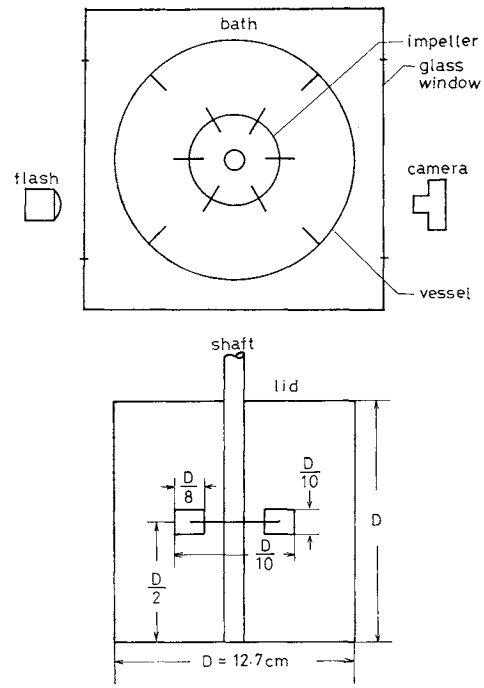

Fig. 2 Schematic diagram of the apparatus

Table 1 Properties of continuous and dispersed phase liquids at 22°C

Continuous phase (water)	
Polyvinylalcohol concentration	0.1 g/*l*
Density	1.00 g/cc
Viscosity	0.97 cp
Dispersed phase (Polystyrene–*o*-xylene solution)	
Polystyrene concentration	0 to 25 wt%
Density	0.879 to 0.922 g/cc
Viscosity	0.78 to 1500 cp
Interfacial tension	22$\pm$0.4 dyne/cm

Table 2 Experimental conditions

Impeller speed	n_r	150–820 rpm
Reynolds number	$\rho_c n_r L^2/\mu_c$	10^4–6×10^4
Dispersed phase volume fraction	ϕ	less than 0.003
Temperature	—	22$\pm$1°C

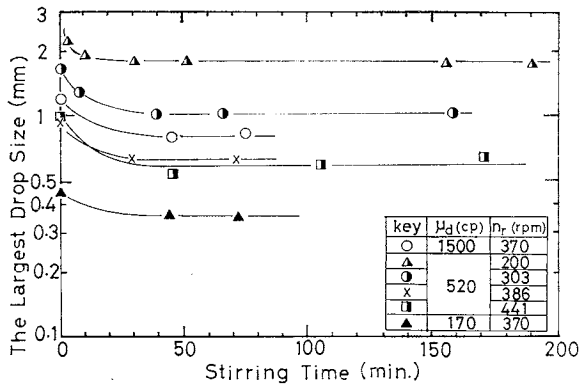

Fig. 3 Change of the largest drop size during stirring time

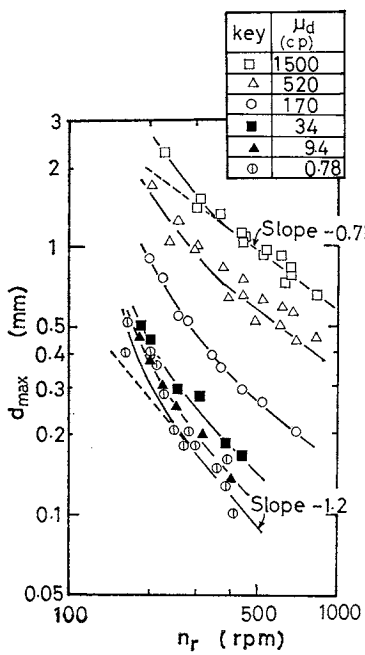

Fig. 4 Effect of impeller speed on the maximum drop size

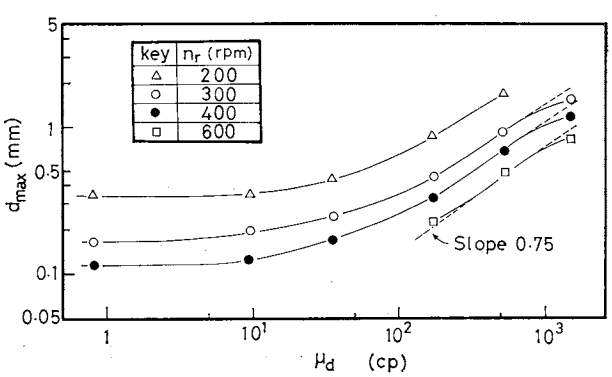

Fig. 5 Effect of dispersed-phase viscosity on the maximum drop size

capillary viscometer or a rotating viscometer. Impeller speeds were above 150 rpm in order to permit impeller Reynolds number greater than 10^4.

Photographs of the dispersion were taken at appropriate intervals during each run. The negatives were projected onto frosted glass screen and then the drop size measurements were made by hand from the reflections using slide calipers. A minimum count of 300 drops was necessary to obtain accurate drop size distribution[1]. The largest drop sizes were defined as drop sizes at which tails of the distributions on large side converge to zero.

3. Experimental Results and Discussion

A plot of the diameter of the largest drop against stirring time is shown in **Fig. 3**. It is apparent from Fig. 3 that the size of the largest drop obtained under each experimental condition reaches a constant value when the system is agitated for more than 40 minutes. Therefore, in this work we adopted the largest drop size obtained after more than 40 minutes in stirring time as the maximum stable drop size d_{max}, because dispersed phase volume fraction ϕ at each run is small enough to neglect the effect of coalescence[8].

3. 1 Effect of impeller speed

Figure 4 shows logarithmic-scale plots of d_{max} vs. n_r. The solid curves are drawn through the data for the same dispersed-phase viscosity. The upper broken line shows the slope of -0.75 predicted from Eq. (30) and the lower broken line the slope of -1.2 predicted from Eq. (5). At impeller speeds above 300 rpm, the data for μ_d larger than 520 cp are well correlated with lines of theoretical slope -0.75 and those smaller than 34 cp with lines of theoretical slope -1.2. However, the data show a curvature tending toward higher slopes independently of μ_d as the impeller speed is decreased below 300 rpm. It should be noted that this tendency appears not only in the small μ_d region as observed by some investigators[5,9,10] but also in the large μ_d region. Therefore, this is caused by a factor which is independent of the change of the dispersed-phase viscosity. On the other hand, it is found that the breakup of drops with sizes near to d_{max} does not occur in every place of an agitated tank but only in the limited place where the local energy dissipation rate is the largest. The distribution of ε in a tank may be affected by changing the impeller speed in the vicinity at the Reynolds number of about 10^4. Therefore, the discrepancy between theoretical and experimental d_{max} in the region of low impeller speed depends on a certain change of the distribution of ε, that is, the approximation of ε by Eq. (4).

3. 2 Effect of dispersed-phase viscosity

The values of d_{max} at each impeller speed are read out from the solid curves in Fig. 4 and then plotted against μ_d in logarithmic coordinates in **Fig. 5**. The slopes of all curves drawn through each set of plots are near to zero in the region of μ_d below 10 cp and increases with the increase from 10 to 200 cp in μ_d. In the region of μ_d above 200 cp the slopes are in good agreement with the theoretical slope of 0.75 which is

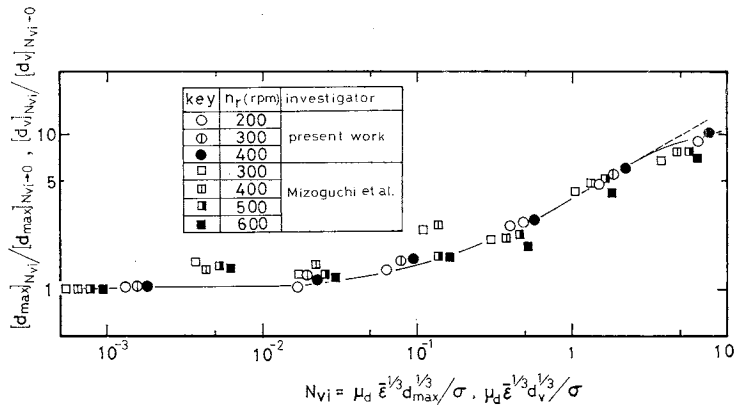

Fig. 6 Correlation of the data by means of the model

predicted from Eq. (29) or from Eq. (30). But when μ_d approaches about 1500 cp, the slopes of all the curves become smaller than the value of 0.75. Although this disagreement between experiments and the model cannot be interpreted quantitatively, it may be caused by the following fact. When μ_d is relatively small, a deformed drop will be quickly restored to a spherical shape in real turbulence for each interval between turbulent fluctuations; that is, a drop will oscillate about spherical equilibrium shape. In this case, the deformation of a drop will be successfully represented by the present model. In contrast to this, when μ_d becomes very larger, it will become difficult for a deformed drop to be restored to a spherical shape for the above-mentioned interval. In this case, even a drop which has a smaller size than that predicted from Eq. (30) will breakup because the drop deformation is enhanced by the subsequent turbulent fluctuations. Therefore, this appears to be a major cause for the disagreement shown in Fig. 5.

3. 3 Correlation of $d_{\max}$ by means of the present model

If Eq. (27) is divided by Eq. (3) under the condition that $\rho_c \varepsilon^{2/3}/\sigma$ is constant, the following equation is obtained.

$$[d_{\max}]_{N_{vi}}/[d_{\max}]_{N_{vi}\to 0}=(1+f(N_{vi}))^{0.6} \tag{31}$$

where $[d_{\max}]_{N_{vi}}$ represents the maximum drop size at N_{vi} and $[d_{\max}]_{N_{vi}\to 0}$ that at $N_{vi}\to 0$.

Equation (31) makes clear the effect of the dispersed-phase viscosity because the ratio of the maximum drop sizes depends only on N_{vi}.

In the present experiments, ρ_c and σ are constant and $\rho_c \varepsilon^{2/3}/\sigma$ is also constant at a constant impeller speed. The maximum drop sizes at μ_d of 0.78 cp for each impeller speed can be used as $[d_{\max}]_{N_{vi}\to 0}$. The ratios of the maximum drop sizes, that is, the values of the left-hand side in Eq. (31), are obtained from Fig. 4 and they are plotted against the viscosity group N_{vi} on logarithmic coordinates in **Fig. 6**. The broken line represents the following relation which is derived from Eqs. (26) and (31).

$$\lim_{N_{vi}\to\infty} \frac{[d_{\max}]_{N_{vi}}}{[d_{\max}]_{N_{vi}\to 0}}=\text{const. } N_{vi}^{0.6} \tag{32}$$

In this figure the present data fall on a single curve as predicted from Eq. (31). It should be noted that the data contain those at n_r of 200 rpm, where the larger effect of n_r on $d_{\max}$ is observed, as shown in Fig. 4, and that this effect of n_r is removed by taking the ratio of the maximum drop sizes. The slope of the curve in the range of N_{vi} near 10 becomes smaller than the value of 0.6 and this, of course, corresponds to the decrease of the slopes in the range of μ_d near 1500 cp, in Fig. 5. The data, except for the high dispersed-phase viscosity range, are well correlated by Eq. (31) in which $f(N_{vi})$ is approximated as follows:

$$f(N_{vi})=9N_{vi} \tag{33}$$

The data* of Mizoguchi *et al.*[5] were also plotted in Fig. 6 by using the volume-average drop diameter d_v instead of $d_{\max}$. It is shown that these data are well correlated by the present model.

Conclusions

This paper presents a more general expression for $d_{\max}$ applicable over a wide range of the dispersed-phase viscosity. Namely, the deformation of a drop in turbulence was represented by the Voigt model, and the equation of the deformation was solved by using the approximation that the dynamic pressure difference acts on a drop periodically; from this solution a formula for $d_{\max}$ was derived by assuming that the breakup of a drop occurs when the magnitude of the deformation reaches a certain critical value. The formula shows that the maximum stable drop size is controlled by two dimensionless groups, N_{We} and N_{vi}. This theoretical result was confirmed experimentally.

Nomenclature

D	= tank diameter
d	= drop diameter
F	= external stress
L	= impeller diameter

* In their experiments, the dispersed phase volume fraction is relatively large, i.e., $\phi=0.1$ but a protecting agent is added to the continuous phase. In this case, coalescence of drops will be prevented remarkably.

N_{vi} = viscosity group, $\mu_d\varepsilon^{1/3}d^{1/3}/\sigma$
N_{We} = Weber number, $\rho_c\overline{u^2}(d)d/\sigma$
n_r = impeller speed
$\Delta P(d,t)$ = dynamic pressure difference
$\overline{\Delta P}$ = average magnitude of $\Delta P(d,t)$
T = mean period of $\Delta P(d,t)$
t = time
$\overline{u^2}(d)$ = mean square of the difference of the velocities at distance d

ε = energy dissipation rate per unit mass
η = Kolmogoroff length, $(\nu_c^3/\varepsilon)^{1/4}$
θ = spring elongation or magnitude of the deformation
μ = viscosity
ν = kinematic viscosity
ω = dimensionless time, t/T
ρ = density
σ = interfacial tension
ϕ = dispersed phase volume fraction

〈Subscripts〉
c = continuous phase
d = dispersed phase
crit = critical
max = maximum
v = volume-average

Literature Cited

1) Brown, D. E. and K. Pitt: *Chem. Eng. Sci.*, **27**, 577 (1972).
2) Hinze, J. O.: *AIChE J.*, **1**, 289 (1955).
3) Hughmark, G. A.: *ibid.*, **17**, 1000 (1971).
4) Konno, M., U. Matsunaga, K. Arai and S. Saito: Preprint of the local meeting of The Soc. of Chem. Engrs., Japan (Muroran), B-8 (1975).
5) Mizoguchi, K., E. Oshima and H. Inoue: *Kagaku Kōgaku*, **38**, 244 (1974).
6) Shinnar, R.: *Fluid Mech.*, **10**, 259 (1961).
7) Sleicher, C. A.: *AIChE J.*, **8**, 471 (1962).
8) Sprow, F. B.: *Chem. Eng. Sci.*, **22**, 435 (1967).
9) Vermeulen, T., G. M. Williams and G. E. Langlois: *Chem. Eng. Progr.*, **51**, 85F (1955).
10) Yamaguchi, I., S. Yabuta and S. Nagata: *Kagaku Kōgaku*, **31**, 275 (1967).

Short Communications

PREDICTION OF SEMIFLUIDIZATION VELOCITY AND PACKED BED FORMATION FOR HETEROGENEOUS MIXTURES IN LIQUID-SOLID SYSTEMS

G. K. ROY AND K. C. BISWAL

Department of Chemical Engineering, Regional Engineering College, Rourkela-769008 (Orissa), India

Introduction

Semifluidization is a new type of solid-fluid contacting technique, which has been reported in the last decade only. It is claimed to be a compromise between the packed and the fluidized bed operations and can be achieved in a conventional fluidizer by incorporating certain modifications to the column construction. The special features of such a bed have been reported in literature[1].

A glance into semi-fluidization literature reveals that various aspects of liquid-solid semi-fluidization viz. the prediction of minimum and maximum semi-fluidization velocities[4-7], packed bed formation[2,3,8], and pressure drop[9] have been exhaustively investigated for closed-cut particles. But information as regards the semi-fluidization behaviour of mixed particles system is very limited[10]. Of late, two correlations have been suggested by one of the authors (Roy) for the prediction of minimum and maximum semi-fluidization velocities[11,12] for heterogeneous mixtures in liquid-solid systems. In this communication a correlation has been proposed for the prediction of semi-fluidization velocity in terms of a few dimensionless groups which influence the system. This will be of practical applicability in determining the relative distribution of particles in the fixed and fluidized sections of a semi-fluidized bed.

Received January 24, 1977. Correspondence concerning this article should be addressed to G. K. Roy.

Experimental Procedure

The experimental set-up used and the procedure followed in the present study has been described in